

Systematic characterization of small inductively coupled radiofrequency coils as MR-visible markers at 1.5T

N. Garnov¹, G. Thörmer¹, W. Gründer², R. Trampel³, M. Moche¹, T. Kahn¹, and H. Busse¹

¹Diagnostic and Interventional Radiology, Leipzig University Hospital, Leipzig, Germany, ²Institute of Medical Physics and Biophysics, University of Leipzig, Leipzig, Germany, ³Max Planck Institute for Human Cognitive and Brain Sciences, Leipzig, Germany

Introduction: MR-guided interventions may benefit from a proper visualization or localization of the deployed instruments. MR-visible markers are usually categorized with respect to their design and method of detection: (1) active markers are signal receivers wired to the scanner, (2) passive ones have no electric components and operate via a positive (paramagnetic agent) or negative (susceptibility) contrast, and (3) semi-active or inductively coupled markers have no connection but involve conducting wires [1]. The goal of this work was to systematically characterize the small inductively coupled solenoid coils and evaluate their suitability as MR-visible markers for interventional applications at 1.5T.

Methods and Materials: The small markers (Fig. 1) consisted of a solenoid coil (inductance 0.06 μ H) with four turns of an insulated copper wire around a water-filled glass tube (inner/outer $\varnothing=2.2/4.0$ mm). An MR-compatible capacitor (ATC, NY) was used to tune the circuit to the resonance frequency (≈ 63.7 MHz) of a 1.5T MRI (Siemens, Germany). The quality factor of the loaded circuit was determined to be ≈ 110 . All measurements were made with the integrated body coil using a plastic bottle filled with NiSO₄ solution as background phantom. Marker imaging was performed with a balanced SSFP sequence (TrueFISP, matrix size=512², FOV/slice thickness=300 mm, TR/TE=6.8/2.8 ms, bandwidth=220 Hz/pixel) in the three standard projections using flip angles (FA) in the 0.1°–90.0° range. The contrast-to-noise ratio was calculated as $CNR=(S_M-S_B)/S_B$, with S_M as maximum marker and S_B as background signal averaged over a fixed ROI.

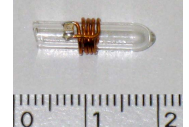


Fig. 1: Resonant RF coil as MR marker.

The spatial dependence of the TrueFISP marker signals (FA=0.3°) was investigated by translating the markers along the x and z axes in the ± 240 mm range around the isocenter. The marker was also placed on a custom-made rotary mount (positioned horizontally) to measure the angular dependence of the TrueFISP marker signal (FA=0.3°) as a function of tilt angle θ_{TRA} (between solenoid axis and transverse plane). An existing localization algorithm was used at this stage to evaluate the suitability for an automatic detection algorithm [2].

Inductive heating of the marker coils during RF exposition was measured to assess potential safety hazards. The temperatures were monitored with a 4-channel fiber optical thermometer (Fluoroptic 700, Luxtron, CA) with one probe taped on the coil wire and another placed inside the glass tube near the geometrical center of the solenoid. Four different sequences were investigated over a time span of 21 min (1 min baseline, 10 min exposition, 10 min cool down): HASTE (TR/TE=1090/121 ms, FA=150°, SAR=1.93 W/kg), VIBE (TR/TE=3.8/1.4 ms, FA=15°, SAR=0.49 W/kg), TrueFISP with a standard (TR/TE=4.3/2.2 ms, FA=72°, SAR=1.95 W/kg) and with a low flip angle (TR/TE=9.7/4.2 ms, FA=2°, SAR<0.001 W/kg). Measurements were performed at an ambient temperature of $\approx 24^\circ\text{C}$ with the MRI ventilator switched off.

Results: The markers typically imposed as round ($\varnothing=2.2\pm 0.1$ mm, n=10) or oval (2.0 ± 0.1 mm \times 3.1 ± 0.4 mm wide) clearly visible, hyperintense objects (Fig. 2). The highest CNR (≈ 130) on a coronal image was obtained at a flip angle of 0.3° (Fig. 3). During translation along the x and z axes, all marker CNRs were larger than 16 while values around the isocenter were much larger (Fig. 4). For tilt angles θ_{TRA} from 0° to 55° all markers were successfully detected in all views with CNR values above 7.5 (Fig. 5). Under RF exposition, heating inside the tube was slightly larger than directly on the outside of the copper wire. The maximum temperature increase ΔT_{max} was $\approx 5.0^\circ\text{C}$ after HASTE and standard TrueFISP exposition and $\approx 1.3^\circ\text{C}$ applying a VIBE sequence. The marker sequence (low-FA TrueFISP) caused no measurable temperature change (Fig. 6). About 10 min after RF exposition, the temperatures had dropped to the starting values (HASTE and VIBE) or showed only a minor difference of 0.5°C (standard TrueFISP). The numerical values for the $\Delta T_{max}/SAR$ ratios were 2.6 (HASTE), 2.7 (VIBE), and 2.6 (standard TrueFISP) in SI units [K·kg/W].

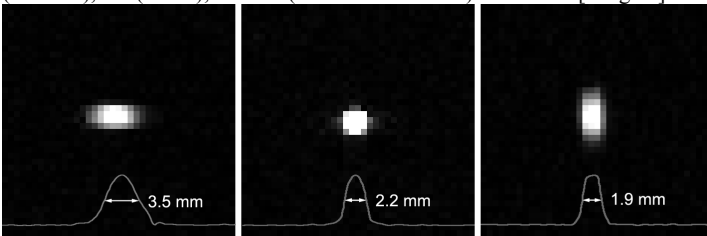


Fig. 2: Typical MR images (detail) in standard views (sagittal, coronal, transverse) and corresponding intensity profiles using a TrueFISP sequence with a flip angle of 0.3°. Numbers indicate full widths at half maximum (FWHM).

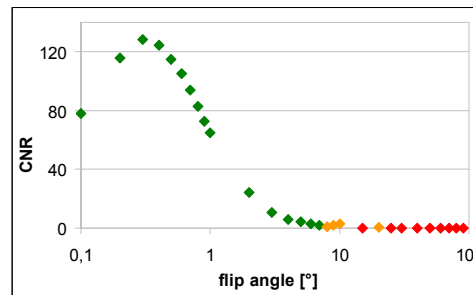


Fig. 3: CNR dependence (logarithmic scale) as a function of flip angle on coronal images. Green, orange, and red symbols denote whether marker signals could be perfectly, partially or not detected with an automatic localization algorithm [2] (also applies to Figs. 4 and 5).

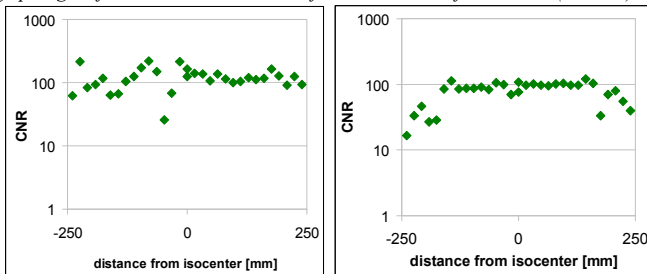


Fig. 4: CNR dependence (logarithmic scale) as a function of marker position on coronal images. **Left:** along z axis. **Right:** along x axis.

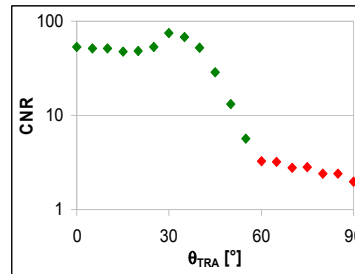


Fig. 5: CNR dependence (logarithmic scale) as a function of tilt angle θ_{TRA} on coronal images.

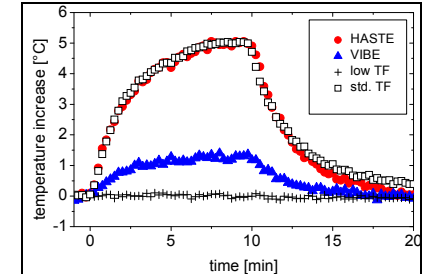


Fig. 6: Temperature evolution in the coil during 10 min RF exposition with different sequences and subsequent 10 min cool down.

Discussion and Conclusions: Within the entire imaging volume, the marker contrast appears to be higher than that of passive markers (of comparable size) [3] and was high enough for automatic detection. The markers may even be operated at larger tilt angles out of the transverse plane (towards B_0). The observed heating is considered negligible for all practical applications outside the body. Because of their simple design and the use of tap water, these markers are relatively easy to implement and could be manufactured as sterile medical disposables. In conclusion, the presented semi-active markers represent a viable solution for various purposes, for example in frameless stereotaxy [4].

References: [1] M. Moche et al., JMRI 2008;27:276 [2] H. Busse et al., JMRI 2007;26:1087 1087 [3] M. Burl et al., MRM 1996;36:491 [4] J.Rachinger et al., Stereot Funct Neuros 2006;84:109